

# Two Zero Mass Matrices and Sterile Neutrinos

---

**Monojit Ghosh <sup>a</sup>, Srubabati Goswami <sup>a</sup>, Shivani Gupta <sup>b</sup>**

<sup>a</sup> *Physical Research Laboratory, Navrangpura, Ahmedabad 380 009, India*

<sup>b</sup> *Department of Physics and IPAP, Yonsei University, Seoul 120-479, Korea*

*Email: monojit@prl.res.in, sruba@prl.res.in, shivani@cskim.yonsei.ac.kr*

**ABSTRACT:** Recent experimental data is indicative of the existence of sterile neutrinos. The minimal scheme that can account for the data and is consistent with cosmological observations is the 3+1 picture which consists of three predominantly active and one predominantly sterile neutrino with the fourth neutrino being heavier than the other three. Within this scheme there are two possibilities depending on whether the three light states obey normal or inverted hierarchy. In this paper we consider the two zero textures of the low energy neutrino mass matrix in presence of one additional sterile neutrino. We find that among 45 possible two zero textures for this case, 15 are consistent with all current observations. Remarkably, these correspond to the two-zero textures of a three active neutrino mass matrix. We discuss the mass spectrum and the parameter correlations that we find in the various textures. We also present the effective mass governing neutrinoless double beta decay as a function of the lowest mass.

---

## Contents

<b>1. Introduction</b>	<b>1</b>
<b>2. Formalism</b>	<b>3</b>
<b>3. Results and Discussions</b>	<b>7</b>
3.1 Results for 3 neutrino mass matrix	7
3.2 Results for 3+1 scenario	9
<b>4. Conclusions</b>	<b>14</b>
<b>5. Acknowledgements</b>	<b>16</b>

---

## 1. Introduction

Neutrino oscillation in standard three flavour picture is now well established from solar, atmospheric, reactor and accelerator neutrinos. The mass squared differences governing these oscillations are  $\sim 10^{-4} \text{ eV}^2$  and  $10^{-3} \text{ eV}^2$ . However, the reported observations of  $\bar{\nu}_\mu - \bar{\nu}_e$  oscillations in LSND experiment [1] and recent confirmation of this by the MiniBooNE experiment [2] with oscillation frequency governed by a mass squared difference  $\sim \text{eV}^2$  cannot be accounted for in the above framework. These results motivate the introduction of atleast one extra neutrino of mass  $\sim \text{eV}$  to account for the three independent mass scales governing solar, atmospheric and LSND oscillations. LEP data on measurement of Z-line shape dictates that there can be only three neutrinos with standard weak interactions and so the fourth light neutrino, if it exists must be a Standard Model singlet or sterile. Recently this hypothesis garnered additional support from (i) disappearance of electron antineutrinos in reactor experiments with recalculated fluxes [3] and (ii) deficit of electron neutrinos measured in the solar neutrino detectors GALLEX and SAGE using radioactive sources [4]. The recent ICARUS results [5] however, did not find any evidence for the LSND oscillations. But this does not completely rule out the LSND parameter space and small active-sterile mixing still remains allowed [6]. Thus, the situation with sterile neutrinos remains quite intriguing and many future experiments are proposed/planned to test these results and reach a definitive conclusion [7].

Addition of one extra sterile neutrino to the standard three generation picture gives rise to two possible mass patterns – the 2+2 and 3+1 scenarios [8]. Of these, the 2+2 schemes are strongly disfavored by the solar and atmospheric neutrino oscillation data [9]. The 3+1 picture also suffers from some tension between observation of oscillations in antineutrino channel by LSND and MiniBooNE and non-observation of oscillations in

the neutrino channels as well as in disappearance measurements. However, it was shown recently in [10] that a reasonable goodness-of-fit can still be obtained. Although introduction of more than one sterile neutrinos may provide a better fit to the neutrino oscillation data [11], the 3+1 scheme is considered to be minimal and to be more consistent with the cosmological data [12]. Very recently combined analysis of cosmological and short baseline (SBL) data in the context of additional sterile neutrinos have been performed in [13, 14]. The analysis in [13] found a preference of the 3+1 scenario over 3+2 while the analysis in [14] shows that the status of the 3+2 scenario depends on the cosmological data set used and the fitting procedure and no conclusive statement can be made regarding whether it is favoured or disallowed. In fact the current cosmological observations of an weakly interacting relativistic "dark radiation" may actually prefer an additional sterile neutrino [15]. If this radiation is attributed to extra neutrino species then the data gives the bound on the number of neutrinos as  $N_{eff} = 4.08 \pm 0.8$  at 95% C.L. [15].

In this paper we consider the structure of the low energy neutrino mass matrices in presence of one extra sterile neutrino. The low energy mass matrix in the flavour basis is now complex symmetric with 10 independent entries and can be expressed in general as,

$$M_\nu = \begin{pmatrix} m_{ee} & m_{e\mu} & m_{e\tau} & m_{es} \\ m_{e\mu} & m_{\mu\mu} & m_{\mu\tau} & m_{\mu s} \\ m_{e\tau} & m_{\mu\tau} & m_{\tau\tau} & m_{\tau s} \\ m_{es} & m_{\mu s} & m_{\tau s} & m_{ss} \end{pmatrix} \quad (1.1)$$

For three flavours the last row and the column would be absent and the mass matrix would contain 6 elements. In the context of three generations, a very remarkable result was obtained in [16] that there can be at the most two zeros in the low energy neutrino mass matrix in the flavour basis. For the three neutrino mass matrix there can be 15 possible two zero texture structures. These are the same as those shown in Table 1 for the four neutrino case after omitting the fourth row and column. Among these, only 7 textures corresponding to the A, B and C class were found to be compatible with the experimental data on neutrino oscillation [16]. Normal Hierarchy (NH) was found to be allowed in all the textures whereas Inverted Hierarchy (IH) and Quasi-Degenerate (QD) solutions were allowed for the B and C classes. Various aspects of the two zero textures in the low energy neutrino mass matrix have been examined in [17, 18]. Recently, this analysis has been redone in [19, 20, 21, 22, 23] to take into account the recent results including the measured values of mixing angle  $\theta_{13}$  by the reactor experiments [24]. The analysis including the latest data and allowing the parameters to vary randomly in their  $3\sigma$  range shows that all 7 textures of the original analysis in [16] remain allowed [23]. However, with the  $1\sigma$  range of parameters the scenarios become more constrained. With the oscillation parameters taken from [25] only A class with NH remain allowed while for oscillation parameters in [26] the textures belonging to  $B_2$  and  $B_4$  classes for IH and C for NH get excluded [23]. This demonstrates that with precise determination of oscillation parameters the allowed scenarios would become more constrained. However, the situation may change altogether in presence of sterile neutrinos.

In this paper, we examine how many two zero textures are allowed by the current oscillation data in the low energy neutrino mass matrix when an extra sterile neutrino is present. We assume the known oscillation parameters are normally distributed with the peak at the best-fit value and  $1\sigma$  error as the width. First we check the status of the two zero texture solutions in the context of three generation mass matrices by this procedure. Then we check how much these conclusions change in the 3+1 scenario with one additional sterile neutrino. We also investigate if any new interesting correlations can be found specially for the sterile mixing angles. Finally, we discuss the changes expected in our result if the mass and mixing parameters are varied randomly in their  $3\sigma$  range instead of varying them in a Gaussian distribution peaked at the best-fit value.

Texture zero implies some of the elements are much smaller than the other elements of the mass matrix. Analysis of texture zeros puts restriction on the nature of the mass spectrum and can give rise to correlations between the mixing angles, masses and CP phases which may be confirmed or falsified by experimental observations. This can often help in understanding the underlying flavour symmetry [27]. In case neutrino mass is generated by seesaw mechanism the texture zeros in the low energy mass matrix can be useful in identifying the possible high scale Yukawa matrices [28, 29, 30].

The plan of the paper goes as follows. In the next section we discuss our formalism. Section III discusses the results. We end in section IV with summary and conclusions.

## 2. Formalism

We consider the 3+1 mass spectrum. This can generate two possible mass orderings. In one case the fourth neutrino is heavier than the other three and in the other case the fourth neutrino is lighter than the other three. LSND/MiniBooNE observations dictate that the mass squared difference of the fourth state with the three other states is  $\sim \text{eV}^2$ . However, the scheme in which the fourth state is lower would be more disfavored from cosmology since there will be three neutrino states with mass  $\sim \text{eV}$  which will contribute to the cosmological energy density. Therefore, we consider the picture in which the fourth state is heavier. Then, there are two possibilities shown in Fig. 1.

1.  $m_1 \approx m_2 < m_3 < m_4$  which corresponds to a normal ordering among the active neutrinos (SNH). This gives

$$m_2 = \sqrt{m_1^2 + \Delta m_{12}^2}, m_3 = \sqrt{m_1^2 + \Delta m_{12}^2 + \Delta m_{23}^2}, m_4 = \sqrt{m_1^2 + \Delta m_{14}^2}.$$

2.  $m_3 < m_2 \approx m_1 < m_4$  corresponding an inverted ordering among the active neutrinos (SIH) with the masses

$$m_1 = \sqrt{m_3^2 + \Delta m_{13}^2}, m_2 = \sqrt{m_3^2 + \Delta m_{13}^2 + \Delta m_{12}^2}, m_4 = \sqrt{m_3^2 + \Delta m_{34}^2}.$$

Here,  $\Delta m_{ij}^2 = m_j^2 - m_i^2$ .

We assume that the charged lepton mass matrix is diagonal and the mixing in the neutrino sector is solely responsible for the leptonic mixing. In the present case, the neutrino mixing matrix,  $V$  can be parametrized in terms of six mixing angles  $(\theta_{13}, \theta_{12}, \theta_{14}, \theta_{23}, \theta_{24}, \theta_{34})$ ,

$A_1$	$A_2$		
$\begin{pmatrix} 0 & 0 & \times & \times \\ 0 & \times & \times & \times \\ \times & \times & \times & \times \\ \times & \times & \times & \times \end{pmatrix}$	$\begin{pmatrix} 0 & \times & 0 & \times \\ \times & \times & \times & \times \\ 0 & \times & \times & \times \\ \times & \times & \times & \times \end{pmatrix}$		
$B_1$	$B_2$	$B_3$	$B_4$
$\begin{pmatrix} \times & \times & 0 & \times \\ \times & 0 & \times & \times \\ 0 & \times & \times & \times \\ \times & \times & \times & \times \end{pmatrix}$	$\begin{pmatrix} \times & 0 & \times & \times \\ 0 & \times & \times & \times \\ \times & \times & 0 & \times \\ \times & \times & \times & \times \end{pmatrix}$	$\begin{pmatrix} \times & 0 & \times & \times \\ 0 & 0 & \times & \times \\ \times & \times & \times & \times \\ \times & \times & \times & \times \end{pmatrix}$	$\begin{pmatrix} \times & \times & 0 & \times \\ \times & \times & \times & \times \\ 0 & \times & 0 & \times \\ \times & \times & \times & \times \end{pmatrix}$
$C$			
$\begin{pmatrix} \times & \times & \times & \times \\ \times & 0 & \times & \times \\ \times & \times & 0 & \times \\ \times & \times & \times & \times \end{pmatrix}$			
$D_1$	$D_2$		
$\begin{pmatrix} \times & \times & \times & \times \\ \times & 0 & 0 & \times \\ \times & 0 & \times & \times \\ \times & \times & \times & \times \end{pmatrix}$	$\begin{pmatrix} \times & \times & \times & \times \\ \times & \times & 0 & \times \\ \times & 0 & 0 & \times \\ \times & \times & \times & \times \end{pmatrix}$		
$E_1$	$E_2$	$E_3$	
$\begin{pmatrix} 0 & \times & \times & \times \\ \times & 0 & \times & \times \\ \times & \times & \times & \times \\ \times & \times & \times & \times \end{pmatrix}$	$\begin{pmatrix} 0 & \times & \times & \times \\ \times & \times & \times & \times \\ \times & \times & 0 & \times \\ \times & \times & \times & \times \end{pmatrix}$	$\begin{pmatrix} 0 & \times & \times & \times \\ \times & \times & 0 & \times \\ \times & 0 & \times & \times \\ \times & \times & \times & \times \end{pmatrix}$	
$F_1$	$F_2$	$F_3$	
$\begin{pmatrix} \times & 0 & 0 & \times \\ 0 & \times & \times & \times \\ 0 & \times & \times & \times \\ \times & \times & \times & \times \end{pmatrix}$	$\begin{pmatrix} \times & 0 & \times & \times \\ 0 & \times & 0 & \times \\ \times & 0 & \times & \times \\ \times & \times & \times & \times \end{pmatrix}$	$\begin{pmatrix} \times & \times & 0 & \times \\ \times & \times & 0 & \times \\ 0 & 0 & \times & \times \\ \times & \times & \times & \times \end{pmatrix}$	

**Table 1:** Allowed two zero textures in the 3+1 scenario. The 15 possible two zero textures of three neutrino case are same as these after omitting the 4th row and column.

three Dirac type CP phases  $(\delta_{13}, \delta_{14}, \delta_{24})$  and three Majorana type CP phases  $(\alpha, \beta, \gamma)$ . The neutrino mass matrix in flavour basis is given by

$$M_\nu = V^* M_\nu^{diag} V^\dagger \quad (2.1)$$

where,  $M_\nu^{diag} = \text{Diag}(m_1, m_2, m_3, m_4)$ .

$V = U.P$  [31] with

$$U = R_{34} \tilde{R}_{24} \tilde{R}_{14} R_{23} \tilde{R}_{13} R_{12} \quad (2.2)$$

where  $R_{ij}$  represent rotation in the  $ij$  generation space, for instance:

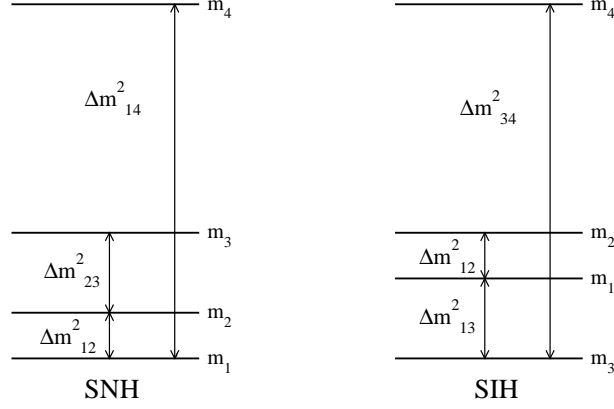


Figure 1: The allowed 3+1 mass ordering

$$R_{34} = \begin{pmatrix} 1 & 0 & 0 & 0 \\ 0 & 0 & 1 & 0 \\ 0 & 0 & c_{34} & s_{34} \\ 0 & 0 & -s_{34} & c_{34} \end{pmatrix}, \quad \tilde{R}_{14} = \begin{pmatrix} c_{14} & 0 & 0 & s_{14}e^{-i\delta_{14}} \\ 0 & 1 & 0 & 0 \\ 0 & 0 & 1 & 0 \\ -s_{14}e^{i\delta_{14}} & 0 & 0 & c_{14} \end{pmatrix}$$

with  $s_{ij} = \sin\theta_{ij}$  and  $c_{ij} = \cos\theta_{ij}$ . The diagonal phase matrix has the form

$$P = \text{Diag}(1, e^{-i\alpha/2}, e^{-i(\beta/2-\delta_{13})}, e^{-i(\gamma/2-\delta_{14})}).$$

The best-fit values and the  $1\sigma$  and  $3\sigma$  ranges of the oscillation parameters in the 3+1 scenario are given in Table 2. One can define three mass ratios

$$x = \frac{m_1}{m_2}e^{i\alpha}, \quad y = \frac{m_1}{m_3}e^{i\beta}, \quad z = \frac{m_4}{m_1}e^{-2i(\gamma/2-\delta_{14})}. \quad (2.3)$$

The two zero textures in the neutrino mass matrix give two complex equations viz.

$$\begin{aligned} M_{\nu(ab)} &= 0, \\ M_{\nu(pq)} &= 0. \end{aligned} \quad (2.4)$$

where  $a, b, p$  and  $q$  can take the values  $e, \mu, \tau$  and  $s$ . The above eqn.(2.4) can be written as

$$U_{a1}U_{b1} + \frac{1}{x}U_{a2}U_{b2} + \frac{1}{y}U_{a3}U_{b3}e^{2i\delta_{13}} + zU_{a4}U_{b4} = 0, \quad (2.5)$$

Parameter	Best fit	1 $\sigma$ range	3 $\sigma$ range
$\Delta m_{12}^2/10^{-5} \text{ eV}^2$ (NH or IH)	7.54	7.32 – 7.80	6.99 – 8.18
$\sin^2 \theta_{12}/10^{-1}$ (NH or IH)	3.07	2.91 – 3.25	2.59 – 3.59
$\Delta m_{23}^2/10^{-3} \text{ eV}^2$ (NH)	2.43	2.33 – 2.49	2.19 – 2.62
$\Delta m_{13}^2/10^{-3} \text{ eV}^2$ (IH)	2.42	2.31 – 2.49	2.17 – 2.61
$\sin^2 \theta_{13}/10^{-2}$ (NH)	2.41	2.16 – 2.66	1.69 – 3.13
$\sin^2 \theta_{13}/10^{-2}$ (IH)	2.44	2.19 – 2.67	1.71 – 3.15
$\sin^2 \theta_{23}/10^{-1}$ (NH)	3.86	3.65 – 4.10	3.31 – 6.37
$\sin^2 \theta_{23}/10^{-1}$ (IH)	3.92	3.70 – 4.31	3.35 – 6.63
$\Delta m_{LSD}^2(\Delta m_{14}^2 \text{ or } \Delta m_{34}^2) \text{ eV}^2$	0.89	0.80 – 1.00	0.6 – 2
$\sin^2 \theta_{14}$	0.025	0.018 – 0.033	0.01 – 0.05
$\sin^2 \theta_{24}$	0.023	0.017 – 0.037	0.005 – 0.076
$\sin^2 \theta_{34}$	–	–	< 0.16

**Table 2:** The experimental constraints on neutrino parameters. The three generation constraints are from global analysis in [25]. The constraints on sterile parameters involving the fourth neutrino are from [13]. The constraint on  $\sin^2 \theta_{34}$  is obtained from [32].

$$U_{p1}U_{q1} + \frac{1}{x}U_{p2}U_{q2} + \frac{1}{y}U_{p3}U_{q3}e^{2i\delta_{13}} + zU_{p4}U_{q4} = 0. \quad (2.6)$$

Solving eqns. (2.5) and (2.6) simultaneously we get the two mass ratios as

$$x = \frac{U_{a3}U_{b3}U_{p2}U_{q2} - U_{a2}U_{b2}U_{p3}U_{q3}}{U_{a1}U_{b1}U_{p3}U_{q3} - U_{a3}U_{b3}U_{p1}U_{q1} + z(U_{a4}U_{b4}U_{p3}U_{q3} - U_{a3}U_{b3}U_{p4}U_{q4})}, \quad (2.7)$$

$$y = -\frac{U_{a3}U_{b3}U_{p2}U_{q2} + U_{a2}U_{b2}U_{p3}U_{q3}}{U_{a1}U_{b1}U_{p2}U_{q2} - U_{a2}U_{b2}U_{p1}U_{q1} + z(U_{a4}U_{b4}U_{p2}U_{q2} - U_{a3}U_{b3}U_{p4}U_{q4})}e^{2i\delta_{13}}. \quad (2.8)$$

The modulus of these quantities gives the magnitudes  $x_m$ ,  $y_m$  while the argument determines the Majorana phases  $\alpha$  and  $\beta$ .

$$x_m = |x|, \quad y_m = |y| \quad (2.9)$$

$$\alpha = \arg(x), \quad \beta = \arg(y). \quad (2.10)$$

Thus, the number of the free parameters is five, the lowest mass  $m_1$  (NH) or  $m_3$  (IH), three Dirac and one Majorana type CP phases. We can check for the two mass spectra in terms of the magnitude of the mass ratios  $x_m$ ,  $y_m$  and  $z_m = |z|$  as,

- SNH which corresponds to  $x_m < 1$ ,  $y_m < 1$  and  $z_m > 1$
- SIH which implies  $x_m < 1$ ,  $y_m > 1$  and  $z_m > 1$

Thus, it is  $y_m$  which determines if the hierarchy among the three light neutrinos is normal or inverted. Note that if the three light neutrinos are quasi-degenerate then we will have  $x_m \approx y_m \approx 1$ . Unlike the three generation case discussed in [17, 18] the lowest mass can not be determined in the four neutrino analysis in terms of  $x_m$  and  $y_m$  since these ratios also depend on  $m_1$  through  $z$ . Thus, we keep the lowest mass as a free parameter. To find out the allowed two zero textures we adopt the following procedure.

We vary the lowest mass randomly from 0 to 0.5 eV. All the five mixing angles in Table 2 (apart from  $\theta_{34}$ ) and the three mass squared differences are distributed normally about the best-fit values with the  $1\sigma$  errors as given in Table 2. The three Dirac and one Majorana type CP phase as well as the remaining mixing angle  $\theta_{34}$  are randomly generated. Then, we use the above conditions to find out which mass spectrum is consistent with the particular texture zero structure under consideration. We also calculate the three mass squared difference ratios

$$\begin{aligned} R_\nu &= \frac{\Delta m_{21}^2}{|\Delta m_{23}^2|} = \frac{1 - x_m^2}{|(x_m^2/y_m^2) - 1|}, \\ R_{\nu 1} &= \frac{|\Delta m_{31}^2|}{\Delta m_{41}^2} = \frac{|1 - y_m^2|}{y_m^2(z_m^2 - 1)}, \\ R_{\nu 2} &= \frac{\Delta m_{21}^2}{\Delta m_{41}^2} = \frac{1 - x_m^2}{x_m^2(z_m^2 - 1)}. \end{aligned} \quad (2.11)$$

The  $3\sigma$  ranges of these three ratios calculated from the experimental data are

$$\begin{aligned} R_\nu &= (0.02 - 0.04), \\ R_{\nu 1} &= (1.98 \times 10^{-3} - 3.3 \times 10^{-3}), \\ R_{\nu 2} &= (0.63 \times 10^{-4} - 1.023 \times 10^{-4}). \end{aligned} \quad (2.12)$$

The allowed textures are selected by checking that they give the ratios within the above range.

### 3. Results and Discussions

In this section we present the results of our analysis. First we briefly discuss the results that we obtain for the two zero textures of the  $3 \times 3$  mass matrices. Next we present the results that we obtain for the 3+1 scenario i.e  $4 \times 4$  mass matrices.

#### 3.1 Results for 3 neutrino mass matrix

For the 3 neutrino case, the lowest mass and the two Majorana phases can be determined from the mass ratios. Hence, the only unknown parameter is the Dirac type CP phase ( $\delta_{13}$ ) which is generated randomly. All the other oscillation parameters are distributed normally, peaked at the best-fit and taking their one sigma error as width. We find that all 7 textures which were allowed previously remain so. However, the textures belonging to A class allow NH whereas for the B class,  $B_1$  and  $B_3$  admit NH and  $B_2$  and  $B_4$  allow IH solutions. Class C gets allowed only for IH. The D, E and F classes remain disallowed. In the 2nd



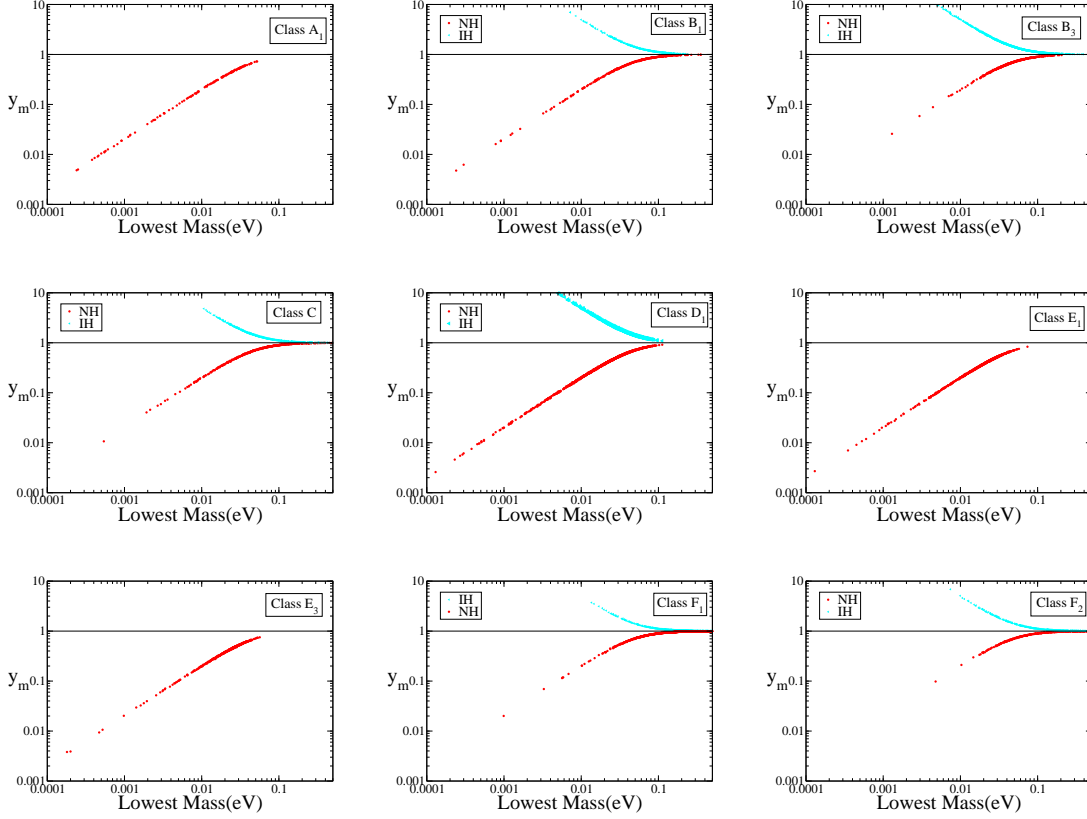


Figure 2: The values of  $y_m$  as a function of the lowest mass ( $m_1$  or  $m_3$ ) for the 3+1 case when the known oscillation parameters are varied in a Gaussian peaked at their respective best-fit values.

column of Table 3 we summarize the results that we obtain for the two zero neutrino mass matrices with three active neutrinos using normal distribution of the oscillation parameters. The results obtained in this case are somewhat different from that obtained using random distribution of oscillation parameters. The reason for the difference stems from the different range of values of the atmospheric mixing angle  $\theta_{23}$  used by these methods. If we assume a Gaussian distribution for  $\sin^2 \theta_{23}$  around its best-fit then there is very less probability of getting the  $3\sigma$  range in the higher octant as these values lie near the tail of the Gaussian distribution. This disallow  $B_2$  and  $B_4$  for NH and  $B_1$  and  $B_3$  for IH [20]. Similarly QD solutions for B class requires  $\theta_{23} \sim \pi/4$  [16] and for a normal distribution of  $\theta_{23}$  with the peak at present best-fit the  $3\sigma$  range extends upto  $\sim 44^\circ$  and there is very little probability of getting values close to  $\pi/4$ . Similarly for the C class NH and QD solutions are allowed only for  $\theta_{23}$  values close to  $\pi/4$  and hence is not admissible when Gaussian distribution of oscillation parameters about the best-fit value is assumed.

Class	3 generation(Random)	3 generation(Gaussian)	3+1 generation (Gaussian)
A	NH	NH	NH
B	NH, IH, QD	NH( $B_1, B_3$ ), IH( $B_2, B_4$ )	NH, IH, QD
C	NH, IH, QD	IH	NH, IH, QD
D	-	-	NH, IH
E	-	-	NH
F	-	-	NH, IH, QD

**Table 3:** The allowed mass spectra in 3 and 3+1 scenarios. The second and third columns give the results for the two zero neutrino mass matrices for three active neutrinos by assuming random and normal distribution of oscillation parameters respectively. The last column gives the allowed spectrum in the for the 3+1 case assuming normal distribution of parameters. For random distribution of oscillation parameters similar mass spectra get allowed although the parameter space is reduced in size. See text for details.

### 3.2 Results for 3+1 scenario

Adding one sterile neutrino, there exist in total forty five texture structures of the neutrino mass matrix which can have two zeros.

- (i) Among these the 9 cases with  $m_{ss} = 0$  are disallowed as the mass matrix element  $m_{ss}$  contains the term  $m_4 U_{s4}^2$  which is large from the current data and suppresses the other terms. Hence,  $m_{ss}$  cannot vanish.
- (ii) There are 21 cases where one has at least one zero involving the mass matrix element of the sterile part i.e  $m_{ks} = 0$  where  $k = e, \mu, \tau$ . This element is of the form,

$$m_{ks} = m_1 U_{k1} U_{s1} + m_2 U_{k2} U_{s2} e^{-i\alpha} + m_3 U_{k3} U_{s3} e^{i(2\delta_{13}-\beta)} + m_4 U_{k4} U_{s4} e^{i(2\delta_{14}-\gamma)}. \quad (3.1)$$

The last term in this expression contains the product  $m_4 U_{s4}$  which is quite large as compared to first three terms and thus, there can be no cancellations. Thus, neutrino mass matrices with one of the zeros in fourth row or column are not viable.

- (iii) The remaining cases are the 15 two zero cases for which none of the sterile components are zero. Thus, these also belong to the two zero textures of the three generation mass matrix. A general element in this category can be expressed as,

$$m_{kl} = m_1 U_{k1} U_{l1} + m_2 U_{k2} U_{l2} e^{-i\alpha} + m_3 U_{k3} U_{l3} e^{i(2\delta_{13}-\beta)} + m_4 U_{k4} U_{l4} e^{i(2\delta_{14}-\gamma)}. \quad (3.2)$$

here,  $k, l = e, \mu, \tau$ . We find all these 15 textures, presented in Table 1 get allowed with the inclusion of the sterile neutrino. This can be attributed to additional cancellations

that the last term in eq. 3.2 induces. Table 3 displays the nature of the mass spectra that are admissible in the allowed textures.

In Fig.2 we present the values of  $y_m$  vs the lowest mass for textures  $A_1, B_1, B_3, C, D_1, E_1, E_3, F_1$  and  $F_2$ . This figure shows that for textures belonging to the A and E classes  $y_m$  remains  $< 1$ . Thus, these classes admit only NH solutions. The textures belonging to the D class allow NH and IH while the B,C,and F classes allow NH, IH and QD mass spectra.

The textures  $A_1 - A_2, B_1 - B_2, B_3 - B_4, D_1 - D_2, E_1 - E_2$  and  $F_2 - F_3$  are related by  $P_{\mu\tau}$  symmetry where for the four neutrino framework  $P_{\mu\tau}$  can be expressed as,

$$P_{\mu\tau} = \begin{pmatrix} 1 & 0 & 0 & 0 \\ 0 & 0 & 1 & 0 \\ 0 & 1 & 0 & 0 \\ 0 & 0 & 0 & 1 \end{pmatrix}$$

in such a way that

$$A_2 = P_{\mu\tau}^T A_1 P_{\mu\tau}.$$

Note that for 3 generation case the angle  $\theta_{23}$  in the partner textures linked by  $\mu - \tau$  symmetry was related as  $\bar{\theta}_{23} = (\frac{\pi}{2} - \theta_{23})$ . However, for the 3+1 case no such simple relations are obtained for the mixing angle  $\theta_{23}$ . The angles  $\theta_{24}$  and  $\theta_{34}$  in the two textures related by  $\mu - \tau$  symmetry are also different. For this case, the mixing angles for two textures linked by  $P_{\mu\tau}$  symmetry are related as

$$\bar{\theta}_{12} = \theta_{12}, \quad \bar{\theta}_{13} = \theta_{13}, \quad \bar{\theta}_{14} = \theta_{14}, \quad (3.3)$$

$$\sin \bar{\theta}_{24} = \sin \theta_{34} \cos \theta_{24}, \quad (3.4)$$

$$\sin \bar{\theta}_{23} = \frac{\cos \theta_{23} \cos \theta_{34} - \sin \theta_{23} \sin \theta_{34} \sin \theta_{24}}{\sqrt{1 - \cos^2 \theta_{24} \sin^2 \theta_{34}}}, \quad (3.5)$$

$$\sin \bar{\theta}_{34} = \frac{\sin \theta_{24}}{\sqrt{1 - \cos^2 \theta_{24} \sin^2 \theta_{34}}}. \quad (3.6)$$

The texture zero conditions together with the constraints imposed by the experimental data allow us to obtain correlations between various parameters specially the mixing angles of the 4<sup>th</sup> neutrino with the other three for the A and E classes. For the B, C, D and F classes one gets constraints on the effective mass governing  $0\nu\beta\beta$ .

In order to gain some analytic insight into the results it is important to understand the mass scales involved in the problem. The solar mass scale is  $\sqrt{\Delta m_{21}^2} \approx 0.009$  eV whereas the atmospheric mass scale is  $\sqrt{\Delta m_{31}^2} \approx 0.05$  eV. Normal hierarchy among the active neutrinos implies  $m_1 \ll m_2 \ll m_3$  corresponding to  $m_1 \lesssim 0.009$  eV. It is also possible that  $m_1 \approx m_2 \ll m_3$  implying  $m_1 \sim 0.009$  eV - 0.1 eV. We call this partial normal hierarchy. IH corresponds to  $m_3 \ll m_1 \approx m_2$ . If on the other hand  $m_1 > 0.1$  eV then  $m_1 \approx m_2 \approx m_3$  which corresponds to quasi-degenerate neutrinos.

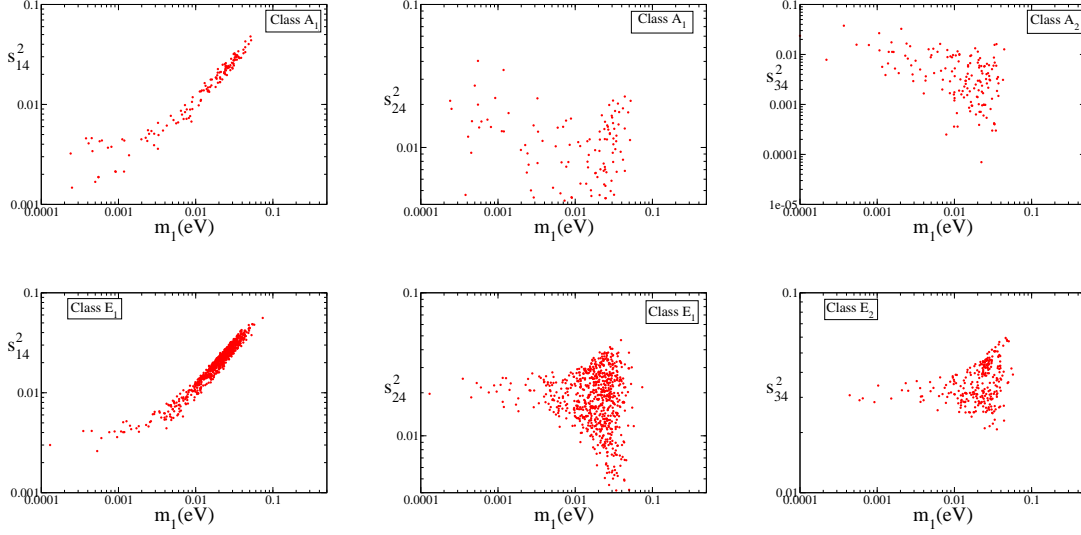


Figure 3: Correlation plots for  $A$  and  $E$  class.

#### • $A$ and $E$ Class

For these classes we find  $y_m$  to be mainly in the range  $> 0.0001$  eV extending up to  $\sim 0.1$  eV. Thus, these classes allow normal hierarchy (full or partial) among the 3 active neutrinos. These classes are characterized by the condition  $m_{ee} = 0$ .  $m_{ee}$  for the four neutrino framework can be expressed as,

$$m_{ee} = c_{12}^2 c_{13}^2 c_{14}^2 m_1 + c_{13}^2 c_{14}^2 e^{-i\alpha} m_2 s_{12}^2 + c_{14}^2 e^{-i\beta} m_3 s_{13}^2 + e^{-i\gamma} m_4 s_{14}^2. \quad (3.7)$$

For smaller values of  $m_1$  and NH the dominant contribution to the magnitude of the above term is expected to come from the last term  $s_{14}^2 \sqrt{\Delta m_{41}^2} \sim 0.022$ . Therefore, very small values of  $m_1$  is less likely to give  $m_{ee} = 0$  for normal hierarchy. However, we get some allowed points in the small  $m_1$  regime which implies smaller values of  $s_{14}^2$ .  $m_{ee}$  can be approximated in the small  $m_1$  limit as,

$$m_{ee} \approx e^{-i\alpha} m_2 s_{12}^2 + e^{-i\beta} m_3 s_{13}^2 + e^{-i\gamma} m_4 s_{14}^2. \quad (3.8)$$

The maximum magnitude of the first two terms is  $\sim 0.003$ . Then using typical values of  $m_4$  ( $\sim 0.9$  eV) from the  $3\sigma$  range, we obtain  $s_{14}^2 \sim (0.003 - 0.004)$  in the small  $m_1$  limit. This is true for all the textures in the  $A$  and  $E$  class. For the  $A_1$  class we also simultaneously need  $m_{e\mu} = 0$ . In the small  $m_1$  limit approximate expression for  $m_{e\mu}$  is

$$m_{e\mu} \approx e^{i(\delta_{14} - \delta_{24} - \gamma)} s_{14} s_{24} m_4 + e^{i(\delta_{13} - \beta)} s_{13} s_{23} m_3 + e^{-i\alpha} c_{12} c_{23} s_{12} m_2, \quad (3.9)$$

and the first term i.e  $m_4 s_{14} s_{24} \sim (0.05 - 0.06) s_{24}$ . While the other terms are of the order  $(0.006 - 0.007)$  which implies  $s_{24}^2 \sim (0.01 - 0.02)$ . This is reflected in the first

and second panels of Fig.3 where the correlation of  $s_{14}^2$  and  $s_{24}^2$  with  $m_1$  is depicted. As  $m_1$  increases the contribution from the first three terms in  $m_{ee}$  increases and  $s_{14}^2$  becomes larger for cancellation to occur. For  $m_{e\mu}$ , this increase in  $s_{14}$  helps to achieve cancellation for higher values of  $m_1$  and therefore  $s_{24}^2$  stays almost the same. Similar argument also apply to the  $E_1$  class which has  $m_{\mu\mu} = 0$ .

For  $A_2$  class, in addition we have  $m_{e\tau} = 0$ . In the limit of small  $m_1$ ,  $m_{e\tau}$  can be approximated as,

$$m_{e\tau} \approx e^{i(\delta_{14}-\delta_{24}-\gamma)} s_{14} s_{34} m_4 + e^{i(\delta_{13}-\beta)} s_{13}^2 m_3 - m_2 e^{-i\alpha} s_{12} c_{12} s_{23}. \quad (3.10)$$

As discussed earlier  $m_{ee} = 0$  implies small  $s_{14}^2 \sim (0.002 - 0.005)$  in the limit of small  $m_1$ . Thus, the contribution from the  $m_4$  term is  $\sim (0.04 - 0.06) s_{34}$ . The typical contribution from the last two terms is  $\sim 0.008$ . This implies  $s_{34}^2$  to be in the range (0.02 - 0.04) for smaller values of  $m_1$ . This is reflected in the third panels of Fig.3 where we have plotted the correlation of  $s_{34}^2$  with  $m_1$ . Since with increasing  $m_1$ ,  $s_{14}$  increases to make  $m_{ee} = 0$ ,  $s_{34}^2$  does not increase further. Similar bounds on  $s_{34}^2$  are also obtained for  $E_2$  class.

As one approaches the QD regime then the terms containing the active neutrino masses starts contributing more. So for higher values of  $m_1$  complete cancellation leading to  $m_{ee} = 0$  even at the highest value of  $s_{14}^2$  is not possible. This feature restricts  $m_1$  to be  $< 0.1$  eV in A class.

Textures belonging to A and E class contains  $m_{ee} = 0$  which is not possible for IH in the 3 generation case since the solar mixing angle is not maximal. In the 3+1 scenario a cancellation leading to  $m_{ee} = 0$  is possible for IH but it requires values of  $s_{14}^2$  in the higher side. It also contains a strong correlation in the Majorana phases. But in the other mass elements these constraints are not satisfied simultaneously and as a result the textures that contain  $m_{ee} = 0$  do not admit inverted hierarchical mass spectrum.

Since  $m_{ee} = 0$ , the effective mass ( $m_{eff} = |m_{ee}|$ ) governing the neutrinoless double beta decay ( $0\nu\beta\beta$ ) is vanishing for these classes.

#### • B, C Classes

In the 3+1 scenario, B and C classes allow all three mass spectra – NH, IH and QD assuming the known oscillation parameters to be normally distributed (cf Table 3). In this case since  $\theta_{23}$  in the textures related by  $\mu - \tau$  symmetry is not correlated in a simple way, the value of this angle not being in the higher octant does not play a significant role as in the 3 generation case. Among these only  $B_1$  allow few points for smaller values of  $m_1$  for NH. For the IH solution, larger number of points are obtained corresponding to the lowest mass  $> 0.01$  eV as is seen from Fig.2. In these textures, for higher values of the lowest mass the active neutrino contribution to the matrix elements are larger and it is easier to obtain cancellations. Hence, textures belonging to these classes show a preference for QD solutions. For these textures the

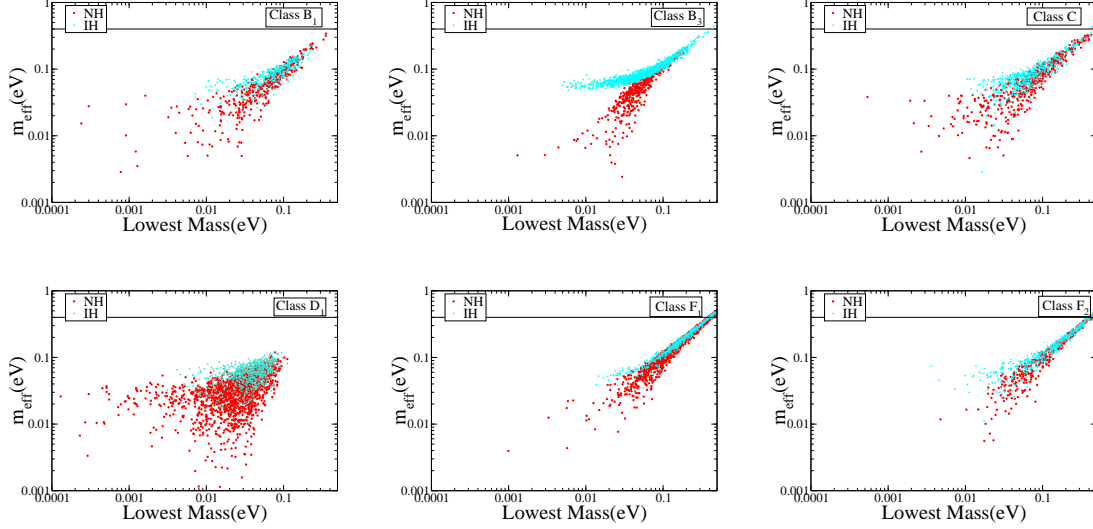


Figure 4: The effective mass governing  $0\nu\beta\beta$  as a function of the lowest mass. The red (dark) points correspond to NH while the cyan (light) points correspond to IH.

effective mass governing  $0\nu\beta\beta$  is non-zero. In the first row of Fig.4 we present the effective mass as a function of the lowest mass for the textures  $B_1$ ,  $B_3$  and C for both NH and IH. These two merge at higher values of the lowest mass corresponding to the QD solution. The effective mass in these textures is  $> 0.002$  eV for NH and  $> 0.02$  eV for IH. If no signal is seen in future  $0\nu\beta\beta$  experiments then large part of the parameter space belonging to these textures can be disfavoured.

- D, F Classes

These two textures are disallowed in the 3 generation case. However for the 3+1 scenario they get allowed. NH is admissible in all the textures belonging to these classes. The reason for this is the following.

In the three active neutrino scenario, the neutrino mass matrix in a  $\mu - \tau$  block has the elements of the order of  $\sqrt{\Delta m_{23}^2} \approx 0.01 eV$  for normal hierarchy. Thus, in general these elements are quite large and cannot vanish [16]. However, in the 3+1 case when there is one additional sterile neutrino, the neutrino mass matrix elements get contribution from the sterile part of the form  $m_4 U_{k4} U_{l4}$  where  $k = e, \mu, \tau$ . This term is almost of the same order of magnitude and thus can cancel the active part, resulting into the possibility of vanishing elements in the  $\mu - \tau$  block. Thus, the zero textures which were disallowed for NH are now allowed by the inclusion of sterile neutrino (3+1 case). In the case of IH,  $m_{\mu\tau}$  element for three active neutrinos is always of the order of  $\sqrt{\Delta m_{23}^2} \approx 0.01 eV$  and thus the textures  $D_1$ ,  $D_2$ ,  $F_2$ ,  $F_3$  which requires  $m_{\mu\tau} = 0$  were not allowed. However, for the 3+1 scenario the extra term coming due to the fourth state helps in additional cancellations and IH gets allowed in these (cf. Table 3). For  $F_1$  class, IH for three active neutrino is disfavoured because of phase

correlations. However, with the additional sterile neutrino this can be evaded making it allowed. In the bottom row of Fig.4 we present the effective mass governing  $0\nu\beta\beta$  for the textures  $D_1$ ,  $F_1$  and  $F_2$  as a function of the lowest mass. The texture  $D_1$  allows lower values of  $m_1$  for NH while for IH the lowest mass is largely  $\gtrsim 0.01$  eV. QD solution is not allowed in D class. For F class more points are obtained in the QD regime. Future experiments on  $0\nu\beta\beta$  would be able to probe these regions of parameter space.

The results presented above are obtained by varying the known oscillation parameters given in Table 2 as distributed normally around their best-fit and with a width given by the  $1\sigma$  range of the parameters. There is a finite probability of getting the points in the  $3\sigma$  range of this Gaussian distribution although more points are selected near the best-fit values. However, note that for some of the parameters the  $3\sigma$  range obtained in this procedure is different from that presented in Table 2. Thus, our results may change if we vary the parameters randomly in their  $3\sigma$  range as we have seen in the 3 generation case. In Fig. 5 we show the allowed values of  $y_m$  as a function of the lowest mass for the case where all the parameters are varied randomly in their  $3\sigma$  range. We find that lower values of the smallest mass get disfavoured by this method. The main reason for this is that if we use the Gaussian method then the allowed  $3\sigma$  range of the mixing angle  $s_{14}^2$  is from (0.002 - 0.048) while that of  $s_{24}^2$  is from (0.001 - 0.06). Thus, smaller values of  $s_{14}^2$  and  $s_{24}^2$  are possible which helps in achieving cancellation conditions for smaller values of  $m_1$  or  $m_3$ . But if the parameters are varied randomly in the  $3\sigma$  range presented in Table 2 then such smaller values of the angles are not allowed and consequently no allowed points are obtained for smaller values of masses. In particular, we obtain  $m_1(\text{NH})$  or  $m_3(\text{IH}) > 0.01$  eV in all the textures. However, main conclusions presented in Table 3 regarding the nature of the allowed mass spectrum for the 3+1 scenario remain unchanged though the allowed parameter space gets reduced. Specially for the A, E and C classes very few points get allowed. Fully hierarchical neutrinos ( $m_1 < m_2 < m_3$ ) are not possible in any of the textures. Textures belonging to the B and F classes give more points in the QD regime. D class allows partial NH or IH.

#### 4. Conclusions

Recent experimental observations make a case for enlarging the scope of three flavour oscillations to include one or more sterile neutrinos with mass around  $\sim 1$  eV. Although induction of more than one sterile neutrino may provide a better fit to the oscillation data the cosmological observations may be more consistent with the three active and one sterile picture with the sterile neutrino being heavier. With the addition of one sterile neutrino the parameter space describing neutrino masses and mixing at low energy increases to include four independent masses, six mixing angles and six phases. The low energy mass matrix in the flavour basis now consists of 10 independent elements as opposed to six elements for the three generation case. It is well known that for the three generation case the neutrino mass matrix in flavour basis can have at the most two zeros. In this work, we

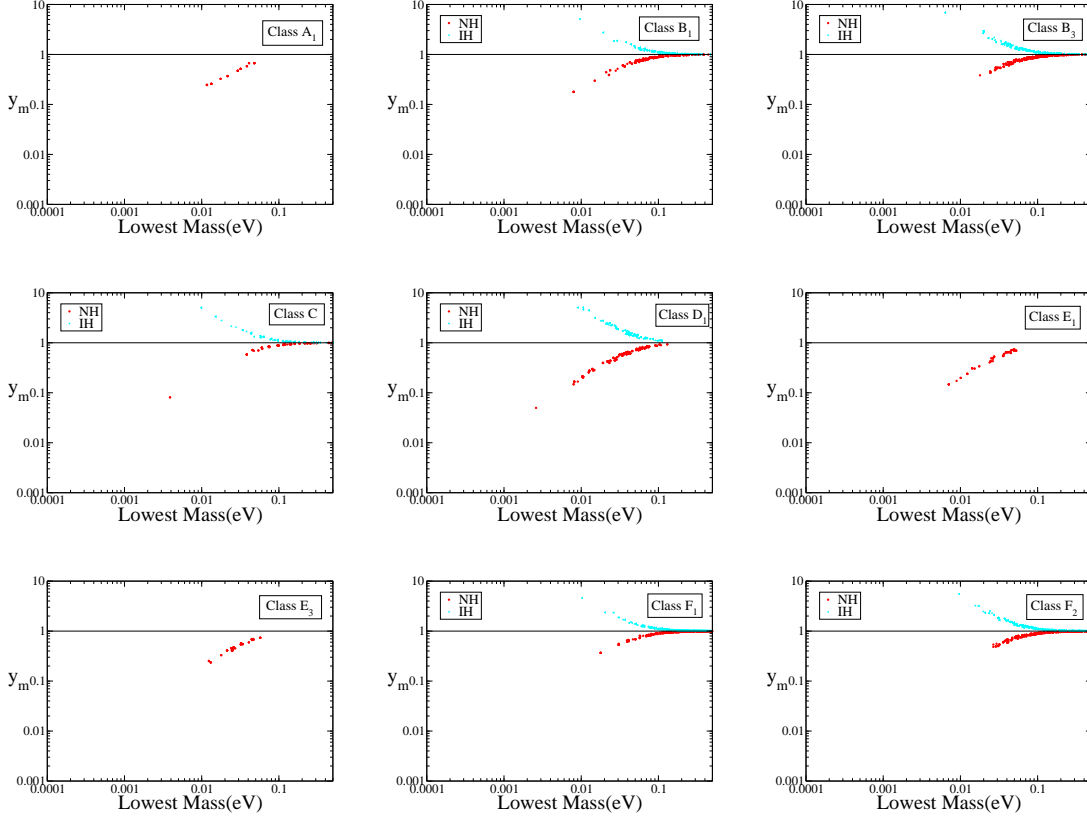


Figure 5: The values of  $y_m$  as a function of the lowest mass when parameters are varied randomly.

have considered the two zero mass matrices in the framework of three active and one sterile neutrino. We find many distinctive features in this case as compared to the three neutrino scenario. For the 3+1 case there can be 45 possible two zero textures as opposed to 15 for the 3 generation case. Among these 45 possible two-zero textures only 15 survive the constraints from global oscillation data. Interestingly these 15 cases are the 15 two-zero textures that are possible for three active neutrino mass matrices. While for the three active neutrino case only 7 of these were allowed addition of one sterile neutrino make all 15 cases allowed as the sterile contribution can be instrumental for additional cancellations leading to zeros. All the allowed textures admit NH. The classes B, C, F also allow IH and QD solutions in addition. The results are summarized in Table 3.

If we vary the mass and mixing parameters normally peaked at the best-fit value and  $1\sigma$  error as the width then we find solutions for smaller values of  $m_1(\text{NH})$  and  $m_3(\text{IH})$ . In this case for the textures with  $m_{ee} = 0$  i.e A class and E class we obtain correlations between the mixing angles  $\sin^2 \theta_{14}$ ,  $\sin^2 \theta_{24}$ ,  $\sin^2 \theta_{34}$  and the lowest mass scale  $m_1$ . For these textures the effective mass responsible for neutrinoless double beta decay is zero. For the other allowed textures we present the effective mass measured in neutrinoless double beta



decay as a function of the smallest mass scale. If however, the known oscillation parameters are varied randomly in their allowed  $3\sigma$  range then although the main conclusions deduced above regarding the allowed mass spectra in various textures remain the same the allowed parameter space reduces in size. In particular, we obtain a bound on the smallest mass as  $m_{\text{smallest}} > 0.01$  eV and completely hierarchical neutrinos are no longer allowed.

In this work we have concentrated on the two zero textures. However it is possible that the neutrino mass matrix in the 3+1 picture may allow the presence of more than two zeros [33]. These results can be useful in probing underlying flavour symmetries and also for obtaining textures of Yukawa matrices in presence of light sterile neutrinos should their existence be confirmed in future experiments.

## 5. Acknowledgements

The authors thank Werner Rodejohann for his involvement in the initial stages of the work and many useful discussions. They would also like to thank Anjan Joshipura for helpful discussions.

## References

- [1] C. Athanassopoulos *et al.* [LSND Collaboration], *Evidence for anti-muon-neutrino to anti-electron-neutrino oscillations from the LSND experiment at LAMPF*, Phys. Rev. Lett. **77**, 3082 (1996) [[arXiv:nuc1-ex/9605003](#)]; **81**, C. Athanassopoulos *et al.* [LSND Collaboration], *Evidence for muon neutrino to electron neutrino oscillations from LSND*, Phys. Rev. Lett. **81**, 1774 (1998) [[arXiv:nuc1-ex/9709006](#)], A. Aguilar-Arevalo *et al.* [LSND Collaboration], *Evidence for neutrino oscillations from the observation of anti-neutrino(electron) appearance in a anti-neutrino(muon) beam*, Phys. Rev. D **64**, 112007 (2001) [[hep-ex/0104049](#)].
- [2] A. A. Aguilar-Arevalo *et al.* [MiniBooNE Collaboration], *A Combined  $\nu_\mu \rightarrow \nu_e$  and  $\bar{\nu}_\mu \rightarrow \bar{\nu}_e$  Oscillation Analysis of the MiniBooNE Excesses*, [[arXiv:hep-ex/1207.4809](#)]; A. A. Aguilar-Arevalo *et al.* [MiniBooNE Collaboration], *A Search for muon neutrino and antineutrino disappearance in MiniBooNE*, Phys. Rev. Lett. **103**, 061802 (2009) [[arXiv:hep-ex/0903.2465](#)].
- [3] G. Mention, M. Fechner, Th. Lasserre, Th. A. Mueller, D. Lhuillier, M. Cribier and A. Letourneau, *The Reactor Antineutrino Anomaly*, Phys. Rev. D **83**, 073006 (2011) [[arXiv:hep-ex/1101.2755](#)].
- [4] C. Giunti and M. Laveder, *Statistical Significance of the Gallium Anomaly*, Phys. Rev. C **83**, 065504 (2011) [[arXiv:hep-ph/1006.3244](#)].
- [5] M. Antonello, B. Baibussinov, P. Benetti, E. Calligarich, N. Canci, S. Centro, A. Cesana and K. Cieslik *et al.*, *Experimental search for the LSND anomaly with the ICARUS LAr TPC detector in the CNGS beam*, [[arXiv:hep-ex/1209.0122](#)].
- [6] C. Giunti, talk in International Symposium on Neutrino Physics and Beyond, September 23-26, 2012, Shenzhen, China.
- [7] K. N. Abazajian, M. A. Acero, S. K. Agarwalla, A. A. Aguilar-Arevalo, C. H. Albright, S. Antusch, C. A. Argüelles and A. B. Balantekin *et al.*, *Light Sterile Neutrinos: A White Paper*, [[arXiv:hep-ph/1204.5379](#)].

- [8] J. J. Gomez-Cadenas and M. C. Gonzalez-Garcia, *Future tau-neutrino oscillation experiments and present data*, Z. Phys. C **71** (1996) 443 [[hep-ph/9504246](#)]. S. Goswami, *Accelerator, reactor, solar and atmospheric neutrino oscillation: Beyond three generations*, Phys. Rev. D **55** (1997) 2931 [[hep-ph/9507212](#)]. N. Okada and O. Yasuda, *A Sterile neutrino scenario constrained by experiments and cosmology*, Int. J. Mod. Phys. A **12** (1997) 3669 [[hep-ph/9606411](#)]. V. D. Barger, T. J. Weiler and K. Whisnant, *Four way neutrino oscillations*, Phys. Lett. B **427** (1998) 97 [[hep-ph/9712495](#)].
- [9] M. Maltoni, T. Schwetz, M. A. Tortola and J. W. F. Valle, *Constraining neutrino oscillation parameters with current solar and atmospheric data*, Phys. Rev. D **67**, 013011 (2003) [[hep-ph/0207227](#)].
- [10] C. Giunti and M. Laveder, *Implications of 3+1 Short-Baseline Neutrino Oscillations*, Phys. Lett. B **706**, 200 (2011) [[arXiv:hep-ph/1111.1069](#)].
- [11] J. Kopp, M. Maltoni and T. Schwetz, *Are there sterile neutrinos at the eV scale?*, Phys. Rev. Lett. **107**, 091801 (2011) [[arXiv:hep-ph/1103.4570](#)]; J. M. Conrad, C. M. Ignarra, G. Karagiorgi, M. H. Shaevitz and J. Spitz, *Sterile Neutrino Fits to Short Baseline Neutrino Oscillation Measurements*, [[arXiv:hep-ex/1207.4765](#)].
- [12] G. Mangano and P. D. Serpico, *A robust upper limit on  $N_{\text{eff}}$  from BBN, circa 2011*, Phys. Lett. B **701**, 296 (2011) [[arXiv:astro-ph.C0/1103.1261](#)].
- [13] C. Giunti and M. Laveder, *3+1 and 3+2 Sterile Neutrino Fits*, Phys. Rev. D **84**, 073008 (2011) [[arXiv:hep-ph/1107.1452](#)].
- [14] S. Joudaki, K. N. Abazajian and M. Kaplinghat, *Are Light Sterile Neutrinos Preferred or Disfavored by Cosmology?*, [[arXiv:astro-ph.C0/1208.4354](#)].
- [15] Z. Hou, R. Keisler, L. Knox, M. Millea and C. Reichardt, *How Massless Neutrinos Affect the Cosmic Microwave Background Damping Tail*, [[arXiv:astro-ph.C0/1104.2333](#)].
- [16] P. H. Frampton, S. L. Glashow and D. Marfatia, *Zeros of the neutrino mass matrix*, Phys. Lett. B **536**, 79 (2002) [[arXiv:hep-ph/0201008](#)].
- [17] S. Dev, S. Kumar, S. Verma and S. Gupta, *Phenomenology of two-texture zero neutrino mass matrices*, Phys. Rev. D **76**, 013002 (2007); [[arXiv:hep-ph/0612102](#)].
- [18] Z. Z. Xing, *Texture zeros and Majorana phases of the neutrino mass matrix*, Phys. Lett. B **530**, 159 (2002) [[arXiv:hep-ph/0201151](#)]; Z. Z. Xing, *A full determination of the neutrino mass spectrum from two-zero textures of the neutrino mass matrix*, Phys. Lett. B **539**, 85 (2002); [[arXiv:hep-ph/0205032](#)]; B. R. Desai, D. P. Roy and A. R. Vaucher, *Three-neutrino mass matrices with two texture zeros*, Mod. Phys. Lett. A **18**, 1355 (2003) [[arXiv:hep-ph/0209035](#)]; S. Dev, S. Kumar, S. Verma and S. Gupta, *CP Violation in Two Texture Zero Neutrino Mass Matrices*, Phys. Lett. B **656**, 79 (2007) [[arXiv:hep-ph/0708.3321](#)]; S. Dev, S. Kumar, S. Verma and S. Gupta, *Phenomenological Implications of a Class of Neutrino Mass Matrices*, Nucl. Phys. B **784**, 103 (2007) [[arXiv:hep-ph/0611313](#)].
- [19] S. Kumar, *Implications of a class of neutrino mass matrices with texture zeros for non-zero  $\theta_{13}$* , Phys. Rev. D **84**, 077301 (2011) [[arXiv:hep-ph/1108.2137](#)].
- [20] H. Fritzsch, Z. -z. Xing and S. Zhou, *Two-zero Textures of the Majorana Neutrino Mass Matrix and Current Experimental Tests*, JHEP **1109**, 083 (2011) [[arXiv:hep-ph/1108.4534](#)].

- [21] D. Meloni and G. Blankenburg, *Fine-tuning and naturalness issues in the two-zero neutrino mass textures*, [[arXiv:hep-ph/1204.2706](#)].
- [22] P. O. Ludl, S. Morisi and E. Peinado, *The reactor mixing angle and CP violation with two texture zeros in the light of T2K*, Nucl. Phys. B **857**, 411 (2012) [[arXiv:hep-ph/1109.3393](#)].
- [23] W. Grimus and P. O. Ludl, *Two-parameter neutrino mass matrices with two texture zeros*, [[arXiv:hep-ph/1208.4515](#)].
- [24] Y. Abe *et al.* [Double Chooz Collaboration], *Indication for the disappearance of reactor electron antineutrinos in the Double Chooz experiment*, Phys. Rev. Lett. **108**, 131801 (2012) [[arXiv:hep-ph/1112.6353](#)]; F. P. An *et al.* [Daya Bay Collaboration], *Observation of electron-antineutrino disappearance at Daya Bay*, Phys. Rev. Lett. **108**, 171803 (2012) [[arXiv:hep-ph/1203.1669](#)]; J. K. Ahn *et al.* [Reno Collaboration], *Observation of electron antineutrino disappearance in the Reno experiment*, Phys. Rev. Lett. **108**, 191802 (2012) [[arXiv:hep-ph/1204.0626](#)].
- [25] G. L. Fogli, E. Lisi, A. Marrone, D. Montanino, A. Palazzo and A. M. Rotunno, *Global analysis of neutrino masses, mixings and phases: entering the era of leptonic CP violation searches*, Phys. Rev. D **86**(2012) 013012 [[arXiv:hep-ph/1205.5254](#)].
- [26] D. V. Forero, M. Tortola and J. W. F. Valle, *Global status of neutrino oscillation parameters after Neutrino-2012*, [[arXiv:hep-ph/1205.4018](#)].
- [27] W. Grimus, A. S. Joshipura, L. Lavoura and M. Tanimoto, *Symmetry realization of texture zeros*, Eur. Phys. J. C **36** (2004) 227 [[hep-ph/0405016](#)].
- [28] G. K. Leontaris, S. Lola, C. Scheich and J. D. Vergados, *Textures for Neutrino Mass Matrices*, Phys. Rev. D **53**, 6381 (1996) [[arXiv:hep-ph/9509351](#)]; S. M. Barr and I. Dorsner, *A general classification of three neutrino models and  $U(e3)$* , Nucl. Phys. B **585**, 79 (2000) [[arXiv:hep-ph/0003058](#)]; A. Kageyama, S. Kaneko, N. Shimoyama and M. Tanimoto, *See-saw realization of the texture zeros in the neutrino mass matrix*, Phys. Lett. B **538**, 96 (2002) [[arXiv:hep-ph/0204291](#)]; P. H. Frampton, S. L. Glashow and T. Yanagida, *Cosmological sign of neutrino CP violation*, Phys. Lett. B **548**, 119 (2002) [[arXiv:hep-ph/0208157](#)];
- [29] R. Barbieri, T. Hambye and A. Romanino, *Natural relations among physical observables in the neutrino mass matrix*, JHEP **0303**, 017 (2003) [[arXiv:hep-ph/0302118](#)]; A. Ibarra and G. G. Ross, *Neutrino phenomenology: The case of two right-handed neutrinos*, Phys. Lett. B **591**, 285 (2004) [[arXiv:hep-ph/0312138](#)]; S. Chang, S. K. Kang and K. Siyeon, *Minimal seesaw model with tri/bi-maximal mixing and leptogenesis*, Phys. Lett. B **597**, 78 (2004) [[arXiv:hep-ph/0404187](#)]; A. Watanabe and K. Yoshioka, *Minimal archi-texture for neutrino mass matrices*, JHEP **0605**, 044 (2006) [[arXiv:hep-ph/0601152](#)];
- [30] W. L. Guo, Z. Z. Xing and S. Zhou, *Neutrino masses, lepton flavor mixing and leptogenesis in the minimal seesaw model*, Int. J. Mod. Phys. E **16**, 1 (2007) [[arXiv:hep-ph/0612033](#)]; G. C. Branco, D. Emmanuel-Costa, M. N. Rebelo and P. Roy, *Four Zero Neutrino Yukawa Textures in the Minimal Seesaw Framework*, Phys. Rev. D **77**, 053011 (2008) [[arXiv:hep-ph/0712.0774](#)]; S. Goswami and A. Watanabe, *Minimal Seesaw Textures with Two Heavy Neutrinos*, Phys. Rev. D **79**, 033004 (2009) [[arXiv:hep-ph/0807.3438](#)]; S. Goswami, S. Khan and A. Watanabe, *Hybrid textures in minimal seesaw mass matrices*, [[arXiv:hep-ph/0811.4744](#)]; S. Goswami, S. Khan and W. Rodejohann, *Minimal Textures in Seesaw Mass Matrices and their low and high Energy Phenomenology*, Phys. Lett. B **680**, 255 (2009) [[arXiv:hep-ph/0905.2739](#)].

- [31] S. Goswami and W. Rodejohann, *Constraining mass spectra with sterile neutrinos from neutrinoless double beta decay, tritium beta decay and cosmology*, Phys. Rev. D **73** (2006) 113003 [[hep-ph/0512234](#)].
- [32] T. Schwetz, talk at the conference Sterile Neutrinos at Crossroads, Virginia Tech, USA, 2011.
- [33] M. Ghosh, S. Goswami, S. Gupta, work in progress.